



A robust unscented Kalman filter and its application in estimating dynamic positioning ship motion states

Xiuyan Peng¹ · Biao Zhang¹ · Lihong Rong^{1,2}

Received: 27 May 2018 / Accepted: 16 January 2019 / Published online: 29 January 2019
© The Japan Society of Naval Architects and Ocean Engineers (JASNAOE) 2019

Abstract

Estimating dynamic positioning ship motion states is complex if the measured nonlinear motion data have outlying data caused by faulty sensors or ocean environmental noises. To overcome the adverse effects of sensor outliers, we developed a modified unscented Kalman filter (MUKF) algorithm. An outlier detection function was first established to spot the outliers in the measurement and then embedded into the regular unscented Kalman filter (UKF) algorithm to modify the covariance of measurement noise for obtaining smooth changes of the filter gain. To verify the developed MUKF algorithm, two dynamic positioning ship motions were simulated for estimating ship motion states in the presence of measurement outliers. Four outlier scenarios with different extents of sensor faults, different points at which the outlier occurred, and outlier duration during the ship motion course were simulated. The estimated values were compared with the theoretical ones. Additional parameter sensitivity was then performed to verify the stability and convergence performance of the developed MUKF algorithm. The results estimated by the robust MUKF were accurate and reliable, regardless of the outlier scenario, indicating the robustness of the MUKF algorithm to reduce the influence of outliers on the estimation of dynamic positioning ship motion states. The implications of this study are also discussed and presented.

Keywords State estimation · Ship motion states · Outlier · Faulty sensors · Modified unscented Kalman filter

1 Introduction

Waves can induce motions and accelerations of a ship at sea. Severe motions such as rolling can affect the comfort of the crew and the passengers, as well as the working performance of the equipment and weapon systems. This may raise safety concerns on marine systems. For risk assessments, it is thus important to carry out real-time measurement and accurate and robust estimation of ship motion states. Measuring ship motion is also helpful to estimate the characteristics of sea wave [1] that can greatly affect marine operations.

Variables associated with measuring ship motion usually contain statistical noise and some inaccuracies due to the interference caused by environmental factors such as winds and waves. Sea state estimation (i.e., wave spectrum estimation) is thus important to evaluate a vessels' performance and thus assist the navigation and operation of a ship [2]. In addition, good data filtering is thus necessary to analyze the noisy data and extract useful ship or sea state information to produce accurate estimates of required ship state variables [3], such as position, velocity, and acceleration. This ship motion has been known to be nonlinear and dynamic by nature [4–6].

As a technique for estimating a ship's motion state, the Kalman filter (KF) produces an optimal estimation of a linear Gaussian system [7] and has numerous applications such as signal processing [8], marine navigation [9], mobile vehicle tracking, navigation, and control [10]. To extend the KF to a nonlinear system, many nonlinear Kalman-type filters have been developed by generating a Gaussian approximation to the distribution of the posterior state. Of these filters, the unscented Kalman filter (UKF) algorithm, based on the unscented transformation, was proposed and has been applied widely for various nonlinear systems in

✉ Biao Zhang
zhangbiao@hrbeu.edu.cn

Xiuyan Peng
pengxiuyan@hrbeu.edu.cn

Lihong Rong
ronglh@hrbeu.edu.cn

¹ College of Automation, Harbin Engineering University, Harbin 150001, China

² College of Information Technology, Heilongjiang Bayi Agricultural University, Daqing 163319, China

practice [11–13], including ship steering applications and various tracking control applications [14, 15]. The UKF is relatively easy to implement in real-time applications to perform appropriate estimations. For example, Peng et al. [15] presented an UKF-based tracking controller for online modelling of the dynamic states and model uncertainty of underactuated surface ships. The simulations showed that the UKF could be applied to update the estimation of the uncertain parameters online to avoid the parameters' drift caused by the time-varying added mass matrices.

However, factors such as sensor noise, measurement sensor malfunction, and unanticipated disturbances like severe tornados in the ocean environment can cause the measurement of ship motion with outlying data that have values much higher or lower than the normal measured data. The presence of outliers could significantly affect the ship state estimation [16]. Thus, it is important to detect and isolate the sensor faults for correctly operating sensor-based ship state estimation system, such as Sea Sense system [6, 17]. For example, Lajic et al. [6, 17] showed onboard sensor fault detection and isolation for in-service monitoring and decision support systems. Note that ship state estimation is an approximate calculation of the ship state, i.e., ship motion values such as ship displacements in different directions at specific motion time.

Processed by the UKF, the abnormal outlying pattern could yield a divergence of linear or nonlinear filter algorithm and thus a biased and unsatisfactory state estimation because the UKF is not robust against a non-Gaussian environment with outliers. Thus, it is crucial to develop a robust technique for ship state estimation in the presence of measurement outliers. Researchers have attempted to develop adaptive Kalman or other robust filters to detect outliers [18, 19] and decrease or eliminate the influence of outliers [20–27]. However, the system model is still linear and not able to illuminate the influence of outliers in a nonlinear dynamic system. Also, those filters are typically difficult to implement and may require expensive computations.

Therefore, the interference of outliers on the state estimation of a ship's nonlinear motion system should be further studied. Durovic and Kovacevic [28] developed a modified KF with an M-estimator to improve the performance of the state estimation while a priori noise and significant dynamical model errors are present. Data samples were assigned weights that represent their contribution to the hidden state estimates at each step. However, these weights, as some heuristic function of the data, might be difficult to be assigned proper threshold parameters that produce optimal performance [29]. Robust statistical procedures have also been used to detect the outlying data points and reduce their influence on the final estimation [30]. If the detected observation differs significantly from its estimated value, then it will be spotted and discarded, requiring manual parameter tuning. Using the statistical methodology, however, it may be

challenging to distinguish an outlier from a relatively natural deviation.

This paper proposes a robust state estimation solution using a modified UKF (MUKF) by incorporating an outlier detection function to spot outliers in the measured dynamic positioning ship motion data and decrease the influence of the outliers on the estimation of ship motion states. As the ship motion is nonlinear and dynamic in practice, the three-DOF including surge, sway, and yaw was considered to meet the dynamic position application requirement. Simulated outliers with different noise scenarios caused by measurement sensor malfunction and measurement noises were effectively detected without the need for manual parameter tuning, and the covariance of the noises was corrected. The MUKF was then compared with the UKF regarding the accuracy of their respective state estimations. The purpose of this study was to understand the influence of outliers on the estimation of dynamic positioning ship motion states and attempt to provide an alternative algorithm for state estimation in a nonlinear system with outlying data.

2 Ship motion model

2.1 Kinematical and motion equations

A ship at sea moves in six degrees of freedom (six-DOF): heave, sway, surge, roll, pitch, and yaw. Our study verifies the developed MUKF using motion data from sway, surge and yaw, all of which are important for a ship dynamic positioning system which normally requires these three DOFs (sway, surge, and yaw) [31, 32]. To describe ship motion, the earth-fixed and the body-fixed coordinate systems are intensively used as reference coordinate systems [33–35] and are thus employed in this paper.

In the body-fixed frame, the moving coordinate system XYZ is fixed to the ship, and the origin O is set to the ship's center of gravity. The alongship displacement (surge), athwartship displacement (sway), and rotational displacement (yaw) are represented by x , y , and ψ , respectively. The corresponding position vector is defined as $\eta = [x, y, \psi]^T$. By decomposing the velocities, the velocity in the surge, sway, and yaw is obtained as u , v , and r , respectively. The corresponding velocity vector is defined as $v = [u, v, r]^T$. The ship motion model is then described as:

$$\dot{\eta} = J(\psi)v, \quad (1)$$

where $J(\psi)$ is a state-dependent transformation matrix of the form:

$$J(\psi) = \begin{pmatrix} \cos \psi & -\sin \psi & 0 \\ \sin \psi & \cos \psi & 0 \\ 0 & 0 & 1 \end{pmatrix}. \quad (2)$$

Note that $\mathbf{J}(\psi)$ is non-singular for all ψ and that $\mathbf{J}^{-1}(\psi) = \mathbf{J}^T(\psi)$.

In the low-frequency motion range, the equation of ship motion can be expressed as:

$$\mathbf{M}\dot{\mathbf{v}} + \mathbf{D}\mathbf{v} = \boldsymbol{\tau} + \mathbf{J}^T(\psi)\mathbf{b}, \quad (3)$$

where $\boldsymbol{\tau} = [\tau_1 \ \tau_2 \ \tau_3]^T$ is a control vector caused by the propulsion system, consisting of τ_1 —control force in surge, τ_2 —control force in sway, and τ_3 —yawing moment. $\mathbf{b} \in \Re^3$ is the disturbance vector, representing all forces and moments due to wind, current, and waves. $\mathbf{M} \in \Re^{3 \times 3}$ is the inertia matrix, and $\mathbf{D} \in \Re^{3 \times 3}$ is the linear damping matrix.

In the high-frequency motion range, ship motion can be simplified as the motion of the simplified second harmonic oscillator [36], which incorporates the damping to the motion and can be expressed as:

$$h(s) = \frac{K_{\omega_i}s}{s^2 + 2\zeta_i\omega_{0i}s + \omega_{0i}^2}, \quad (4)$$

where $K_{\omega_i}(i = 1, 2, 3)$ is the gain coefficient related to wave intensity. $\zeta_i(i = 1, 2, 3)$ is the relative damping ratio and generally between 0.05 and 0.2. $\omega_{0i}(i = 1, 2, 3)$ is the dominant wave frequency and related to significant wave heights [37]. s is the eigenvalues of the characteristic equation $s^2 + 2\zeta_i\omega_{0i}s + \omega_{0i}^2$.

Equation (4) can also be written in the state-space form and is represented as:

$$\dot{\xi}_w = \mathbf{A}_w\xi_w + \mathbf{E}_w w_w, \quad (5)$$

$$\eta_w = \mathbf{C}_w\xi, \quad (6)$$

where $\xi_w = [\xi_x, \xi_y, \xi_\varphi, x_w, y_w, \varphi_w]^T$ contains ship position and speed variables in the direction of surge, sway, and yaw. $w_w = [w_{w1}, w_{w2}, w_{w3}]^T$ is the Gaussian white noise with zero mean in the above three directions. η_w represents the surge position, sway position, and yawing angle. \mathbf{A}_w , \mathbf{E}_w , and \mathbf{C}_w are constant coefficient matrixes and written as:

$$\mathbf{A}_w = \begin{bmatrix} 0 & \mathbf{I} \\ \Lambda_{21} & \Lambda_{21} \end{bmatrix}, \quad (7)$$

$$\mathbf{E}_w = \begin{bmatrix} 0 \\ \mathbf{E}_2 \end{bmatrix}, \quad (8)$$

$$\mathbf{C}_w = [0 \ \mathbf{I}], \quad (9)$$

where $\Lambda_{21} = -\text{diag}\{\omega_{01}^2, \omega_{02}^2, \omega_{03}^2\}$, $\Lambda_{22} = -\text{diag}\{2\zeta_1\omega_{01}, 2\zeta_2\omega_{02}, 2\zeta_3\omega_{03}\}$, and $\mathbf{E}_2 = \text{diag}\{k_1, k_2, k_3\}$. k_i is the wave intensity.

2.2 Environmental force and moment model

It is believed that the environmental force \mathbf{b} in Eq. (3) is the combined result due to various environmental factors such as wave drift force, wind, and stream. The environmental force can be regarded as a parameter with slowly changing values in the ship control system and can be modeled as:

$$\dot{\mathbf{b}} = -\mathbf{T}^{-1}\mathbf{b} + \mathbf{E}_b w_b, \quad (10)$$

where $\mathbf{b} \in \Re^3$ represents slowly changing environmental forces and moment. $w_b \in \Re^3$ is a zero-mean Gaussian white noise. $\mathbf{T} \in \Re^{3 \times 3}$ is a diagonal matrix of positive definite time constants. $\mathbf{E}_b \in \Re^{3 \times 3}$ is a diagonal matrix scaling the amplitude of w_b .

2.3 Measurement model

The mathematical model for measuring ship location can be shown as:

$$\mathbf{y} = \boldsymbol{\eta} + \boldsymbol{\eta}_w + \mathbf{v}_k \quad (11)$$

where $\mathbf{y} \in \Re^3$ represents ship state variables. $\boldsymbol{\eta}_w$ represents high-frequency ship position and heading variables. $\boldsymbol{\eta}$ represents ship low-frequency position and heading variables. $\mathbf{v}_k \in \Re^3$ is the measurement noise.

Based on the mathematical model of ship motion shown in Eqs. (1–11), we then can express the state-space form of the ship motion model as:

$$\begin{cases} \dot{\mathbf{x}} = f(\mathbf{x})\mathbf{x} + \mathbf{B}\mathbf{u} + \mathbf{E}\mathbf{w} \\ \mathbf{y} = \mathbf{H}\mathbf{x} + \mathbf{V}_k \end{cases}, \quad (12)$$

$$\text{where } \mathbf{x} = \begin{bmatrix} \xi \\ \boldsymbol{\eta} \\ \mathbf{v} \\ \mathbf{b} \end{bmatrix}, \mathbf{B} = \begin{bmatrix} 0 \\ 0 \\ 0 \\ \mathbf{M}^{-1} \end{bmatrix},$$

$$f(\mathbf{x}) = \begin{bmatrix} \mathbf{A}_w & 0 & 0 & 0 \\ 0 & 0 & \mathbf{J}(\psi) & 0 \\ 0 & 0 & \mathbf{M}^{-1}\mathbf{D} & \mathbf{M}^{-1}\mathbf{J}^T(\psi) \\ 0 & 0 & 0 & -\mathbf{T}^{-1} \end{bmatrix}, \mathbf{u} = \boldsymbol{\tau}, \mathbf{H} = [\mathbf{C}_w \ \mathbf{I} \ 0 \ 0],$$

$$\mathbf{E} = \begin{bmatrix} \mathbf{E}_w & 0 & 0 & 0 \\ 0 & 0 & 0 & 0 \\ 0 & 0 & 0 & 0 \\ 0 & 0 & 0 & \mathbf{E}_b \end{bmatrix}.$$

3 Review of the UKF algorithm

Because the MUKF algorithm developed in this study was based on the regular UKF algorithm, the UKF algorithm is first reviewed and summarized in this section.

Based on Eq. (12), the discrete-time state-space model of ship motion is given by Eq. (13).

$$\begin{cases} \mathbf{x}_k = f(\mathbf{x}_{k-1}, u_{k-1}) + \mathbf{w}_k \\ \mathbf{y}_k = H\mathbf{x}_k + \mathbf{V}_k \end{cases}, \quad (13)$$

where \mathbf{x}_k is the state vector, and u_{k-1} and \mathbf{y}_k are the input and output vectors at time step k . \mathbf{w}_k is the process noise vector with the covariance matrix \mathbf{Q}_k , \mathbf{V}_k is the measurement noise with the covariance matrix \mathbf{R}_k , and H is the observation matrix.

For the nonlinear system described in the Eq. (13), the estimation of state variables can be optimized by the UKF algorithm [6] through the following steps.

Step 1: Initialization.

Given the state vector $\hat{\mathbf{x}}_{k-1}$ and the error covariance matrix \mathbf{P}_{k-1} , the sigma points $\chi_{i,k-1}$ are formulated by:

$$\begin{cases} \chi_{i,k-1} = \hat{\mathbf{x}}_{k-1} & i = 0 \\ \chi_{i,k-1} = \hat{\mathbf{x}}_{k-1} + (a\sqrt{L}\mathbf{P}_{k-1}) & i = 1, \dots, L \\ \chi_{i,k-1} = \hat{\mathbf{x}}_{k-1} - (a\sqrt{L}\mathbf{P}_{k-1}) & i = L + 1, \dots, 2L \end{cases} \quad (14)$$

where the scalar a determines the spread of the sigma points around $\hat{\mathbf{x}}_{k-1}$ and is usually set to a small positive value. $(\sqrt{\mathbf{P}})_i$ denotes the i th column of the square root of the matrix \mathbf{P} .

Step 2: Prediction.

New sigma points are generated through the unscented transformation by transition function $f(\cdot)$ on the old sigma points:

$$\chi_{i,k/k-1} = f(\chi_{i,k-1}, u_{k-1}). \quad (15)$$

The predicted mean and error covariance are, respectively, given by:

$$\hat{\mathbf{x}}_{k/k-1} = \sum_{i=0}^{2L} w_i \chi_{i,k/k-1}, \quad (16)$$

and

$$\mathbf{P}_{k/k-1} = \sum_{i=0}^{2L} w_i (\chi_{i,k/k-1} - \hat{\mathbf{x}}_{k/k-1})(\chi_{i,k/k-1} - \hat{\mathbf{x}}_{k/k-1})^T + \mathbf{Q}_k, \quad (17)$$

where $\chi_{i,k/k-1}$ is the updated sampling point, $\hat{\mathbf{x}}_{k/k-1}$ is the predicted value of a state variable, $\mathbf{P}_{k/k-1}$ is the mean squared error matrix of $\hat{\mathbf{x}}_{k/k-1}$, and w_i is the weight of the sigma points, defined as:

$$\begin{cases} w_i = 1 - \frac{1}{a^2} & i = 0 \\ w_i = \frac{1}{2La^2} & i = 1, \dots, 2L \end{cases}. \quad (18)$$

Step 3: Measurement update.

The measurements of sigma points are given by:

$$\hat{\mathbf{Y}}_{k/k-1} = H(\chi_{i,k/k-1}, \mathbf{u}_{k/k-1}). \quad (19)$$

The weighted mean of the predicted measurements is given by:

$$\hat{\mathbf{y}}_{k/k-1} = \sum_{i=0}^{2L} w_i \hat{\mathbf{Y}}_{k/k-1}. \quad (20)$$

The updated measurement equations of the UKF are given as follows:

$$\mathbf{P}_{yy} = \sum_{i=0}^{2L} w_i (\hat{\mathbf{Y}}_{k/k-1} - \hat{\mathbf{y}}_{k/k-1})(\hat{\mathbf{Y}}_{k/k-1} - \hat{\mathbf{y}}_{k/k-1})^T + \mathbf{R}_k, \quad (21)$$

$$\mathbf{P}_{xy} = \sum_{i=0}^{2L} w_i (\chi_{i,k/k-1} - \hat{\mathbf{x}}_{k/k-1})(\hat{\mathbf{Y}}_{k/k-1} - \hat{\mathbf{y}}_{k/k-1})^T, \quad (22)$$

$$\mathbf{K}_k = \mathbf{P}_{xy} \mathbf{P}_{yy}^{-1}, \quad (23)$$

$$\hat{\mathbf{x}}_k = \hat{\mathbf{x}}_{k/k-1} + \mathbf{K}_k (\mathbf{y}_k - \hat{\mathbf{y}}_{k/k-1}), \quad (24)$$

$$\mathbf{P}_k = \mathbf{P}_{k/k-1} - \mathbf{P}_{xy} \mathbf{P}_{yy}^{-1} \mathbf{P}_{xy}^T, \quad (25)$$

where \mathbf{P}_{yy} is the covariance matrix of the predicted measurement, \mathbf{R}_k is the covariance matrix of measurement noise, \mathbf{P}_{xy} is the covariance matrix between the state and the measurement, \mathbf{K}_k is the filter gain, $\hat{\mathbf{x}}_k$ is the state estimation, and \mathbf{P}_k is the corresponding covariance matrix.

Steps 1–3 were repeated until all the samples were calculated.

4 Modified UKF algorithm

This section presents the MUKF algorithm that aims to estimate state variables with outlying data by embedding a detection function in the UKF framework. This detection function based on statistical information was proposed to automatically identify the outliers.

4.1 Outlier detection function

Based on the definition of an outlier, the measured outlying data would, at least moderately, deviate from the predicted values. Thus, the change of residuals between the measured value and the predicted value, and its corresponding covariance, can be used as key parameters to spot the outlying data.

In this paper, the outlier detection function value η_k is expressed as:

$$\eta_k = \mathbf{e}_k^{*T} [\mathbf{P}_{yy}]^{-1} \mathbf{e}_k^*, \quad (26)$$

where $\mathbf{e}_k^* = (1/\sqrt{n}) \sum_{i=k-n+1}^k \mathbf{e}_i$, n represents the length of sampling, and \mathbf{e}_i is the residual between the measured value and the predicted value and can be regarded as a random variable with standard normal distribution. \mathbf{P}_{yy} can be referred to Eq. (21).

To judge whether there are outliers in the measured data, the following two hypotheses can be introduced:

- Null hypothesis H_0 . The measurement system is working without any fault.
- Alternative hypothesis H_1 . There are faults in the measurement system.

By proposing the above two hypotheses, the outlier detection function value η_k can be reasonably assumed to obey the χ^2 distribution with Z DOF, where Z is the dimension of the residual vector. We then define Eq. (27):

$$P(\chi^2 > \chi_{\alpha,Z}^2) = \alpha, \quad (27)$$

where $\alpha(0 < \alpha < 1)$ is the significance level, and $\chi_{\alpha,Z}^2$ is the chi square threshold value and can be determined from the χ^2 distribution table, given the DOF and level of significance. If the statistical value η_k is no more than the threshold value $\chi_{\alpha,Z}^2$, the null hypothesis H_0 is accepted and the measured data are those without outliers. On the contrary, if the alternative hypothesis H_1 is accepted, the measured data containing outlying data will be analyzed by the MUKF described in Sect. 4.2.

For the study purpose in this paper, note that the Z DOF is 3, the significance level α can be set to a commonly used value of 0.01, and the chi square threshold value $\chi_{\alpha,Z}^2$ is thus 11.345 according to the χ^2 distribution reference table [38]. The influence of significance level and its corresponding threshold $\chi_{\alpha,Z}^2$ value on the estimation performance of the MUKF is discussed in Sect. 7.

4.2 MUKF algorithm

The outlier detection function, used to identify the outlying data, can be incorporated into the UKF algorithm to generate an adaptive MUKF algorithm. When outliers are detected, the actual error will be larger than the theoretical value in the UKF. To produce an accurate estimation of ship motion states, the covariance of measurement noise \mathbf{R}_k in Eq. (21) will be automatically modified to make the real covariance matrix of predicted measurement equal to the theoretical value when no outliers appear in the measured data. This relationship can be expressed:

$$\frac{1}{\varepsilon} \sum_{i=k-\varepsilon+1}^k \mathbf{e}_i \mathbf{e}_i^T = \sum_{i=0}^{2L} w_i (\hat{\mathbf{Y}}_{k/k-1} - \hat{\mathbf{y}}_{k/k-1}) \times (\hat{\mathbf{Y}}_{k/k-1} - \hat{\mathbf{y}}_{k/k-1})^T + \hat{\mathbf{R}}_k \quad (28)$$

So that the filter gain is maintained and thus the state estimation cannot be changed substantially. Based on Eq. (28), the modified \mathbf{R}_k is thus expressed as:

$$\hat{\mathbf{R}}_k = \frac{1}{\varepsilon} \sum_{i=k-\varepsilon+1}^k \mathbf{e}_i \mathbf{e}_i^T - \sum_{i=0}^{2L} w_i (\hat{\mathbf{Y}}_{k/k-1} - \hat{\mathbf{y}}_{k/k-1})(\hat{\mathbf{Y}}_{k/k-1} - \hat{\mathbf{y}}_{k/k-1})^T \quad (29)$$

where ε is the width of the moving window. $\hat{\mathbf{R}}_k$ is the modified covariance matrix of measurement noise. The derived MUKF with modified $\hat{\mathbf{R}}_k$ in Eq. (29) is then used to calculate the filter gain and variables of ship motion states, while other equations are the same as those in the UKF algorithm in Sect. 3. If there are no outliers, Eq. (21) will not be different, and thus the UKF algorithm will still be utilized. Figure 1 presents the working procedures of the iterated MUKF algorithm.

5 Simulations

5.1 Simulation condition

To demonstrate the feasibility and reliability of the MUKF in detecting outliers and decreasing their influence on the estimation of ship motion states, two ships with the dimensions and parameters shown in Table 1 were used in the simulation. Ship 1 is a full-scale ship while Ship 2 is a model with a 1:20 ratio of a real ship. Table 2 presents the inertia matrix and damping matrix of both Ship 1 and Ship 2.

The ships were designed to move from an initial position [0, 0, 0] to a target position [30, 30, 10]. Three-DOF of motion—surge, sway, and yaw—were investigated regarding their state estimation errors.

The main wave frequency, relatively damping coefficient, and wave intensity are, respectively, $\omega_{01} = \omega_{02} = \omega_{03} = 0.8$, $\zeta_1 = \zeta_2 = \zeta_3 = 0.3$, and $k_1 = k_2 = k_3 = 1$.

For initiation, the parameters in the UKF and MUKF algorithms in this study were set to the following:

- The sampling time and period are 0.5 s and 350 s.
- The initial state error and its covariance are $\text{diag}(20, 20, 0.005, 0.001, 0.001, 0.0001)$ and $\text{diag}(20^2, 20^2, 0.005^2, 0.001^2, 0.001^2, 0.0001^2)$, respectively.
- The initial system noise and its covariance are $\text{diag}(0.001, 0.001, 0.001, 0.0001, 0.0001, 0.0001)$ and $\text{diag}(0.001^2, 0.001^2, 0.001^2, 0.0001^2, 0.0001^2, 0.0001^2)$, respectively.
- The initial measurement noise and its covariance are $\text{diag}(0.001, 0.001, 0.001, 0.0001, 0.0001, 0.0001)$ and $\text{diag}(0.001^2, 0.001^2, 0.001^2, 0.0001^2, 0.0001^2, 0.0001^2)$, respectively.

Fig. 1 Flow chart of the MUKF algorithm

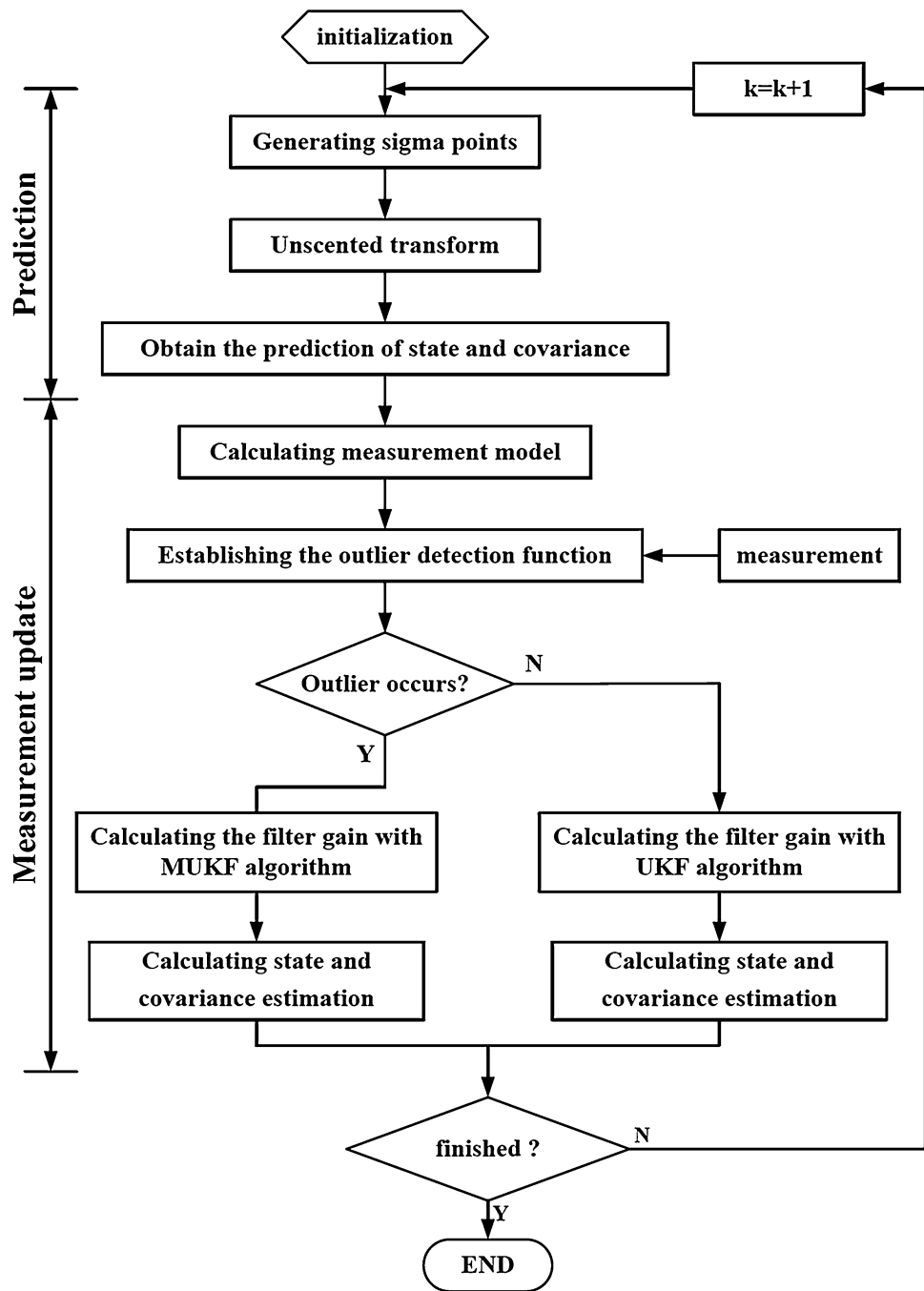


Table 1 Parameters of two ships used in this study

Parameters	Ship 1	Ship 2
Length	175 m	3.75 m
Beam	25.4 m	0.86 m
Height	15.5 m	0.40 m
Draft	9.5 m	0.33 m
Displacement tonnage	24,609.62 t	0.75 t

- The width of the moving window in Eq. (29) was set as 2 (i.e., two continual sampling points).

5.2 Outliner scenario and evaluation parameter

Considering the time at which outliers occur and the duration and extent of each outlier, there are uncountable scenarios that could appear in the measurement data. For ship motions, the main outlier scenarios are zero measurement

Table 2 Inertia matrix and damping matrix of Ship 1 and Ship 2

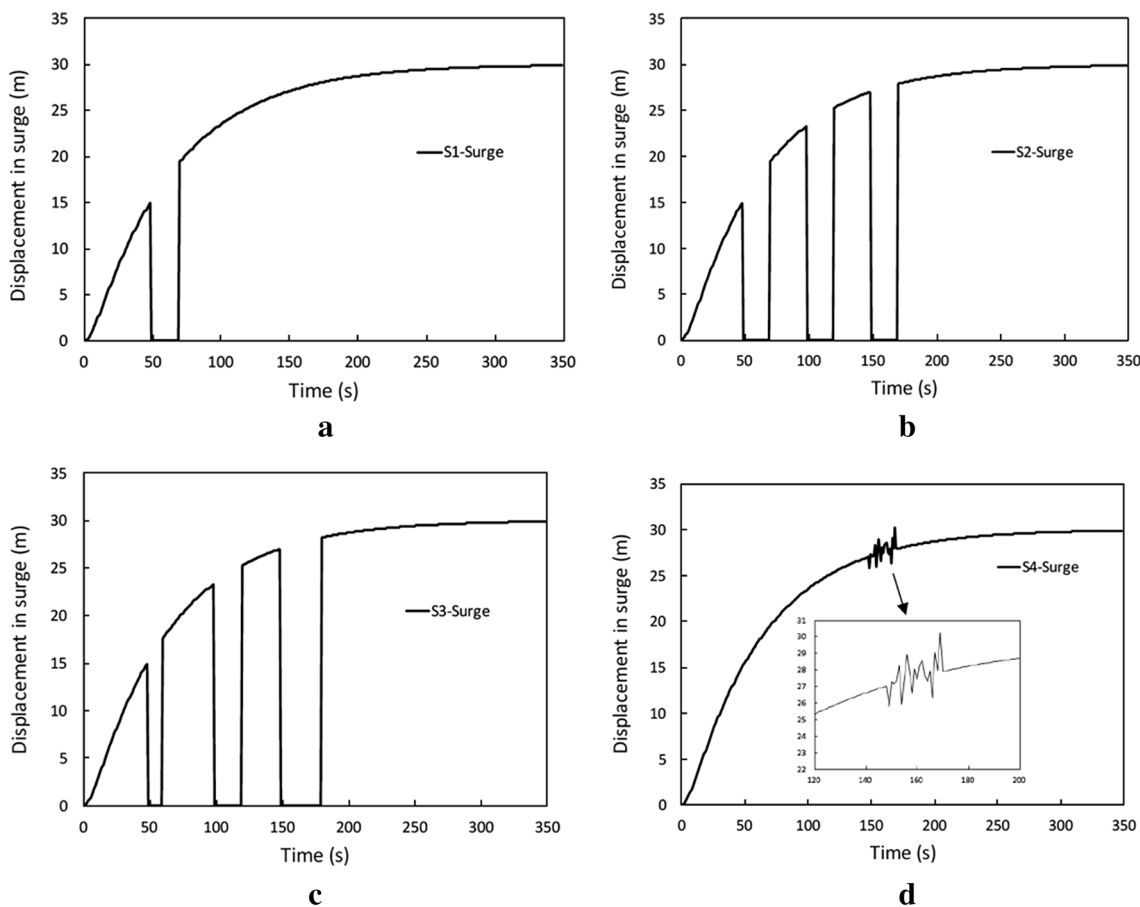
	Inertia matrix	Damping matrix
Ship 1	$M_1 = 10^8 \times \begin{bmatrix} 0.2642 & 0 & 0 \\ 0 & 0.3346 & 0.1492 \\ 0 & 0.1492 & 652.09 \end{bmatrix}$	$D_1 = \begin{bmatrix} 22204 & 0 & 0 \\ 0 & 222040 & -1774600 \\ 0 & -1774600 & 7.1506 \times 10^8 \end{bmatrix}$
Ship 2	$M_2 = \begin{bmatrix} 748.7 & 0 & 0 \\ 0 & 189.1 & 93.8 \\ 0 & 39.6 & 660.4 \end{bmatrix}$	$D_2 = \begin{bmatrix} 12.3 & 0 & 0 \\ 0 & 59.7 & 3 \\ 0 & 3 & 7.1 \end{bmatrix}$

Table 3 Scenarios of sensor faults and their outliers for each ship

Scenario	Extent of sensor faults	Occurring time of each outlier (s)	Duration of each outlier (s)
S1	Complete failure (100%)	50	20
S2		50, 100, 150	20
S3		50, 100, 150	10, 20, 30
S4	Incomplete failure with measurement noise	150	20

outliers when measurement sensors are completely faulty and measurement noise outliers when the measurement contains large noise.

We simulated sensor-induced error by manipulating the output state value in Eq. (13) as zero if a sensor totally malfunctions due to power outage or other serious issues. On the other hand, if sensor signals are noised by wind, wave, or current, the value can be simulated with a high value. Table 3 presents four simulated outlier examples with different extents chosen to be representative of the innumerable outlier scenarios in this study.

**Fig. 2** Plots of displacement in surge in **a** S1, **b** S2, **c** S3, and **d** S4

In the first three scenarios, the sensor was simulated to be completely faulty at the elapsed time of 50 s with the duration of 20 s (S1); at the elapsed time of 50 s, 100 s, and 150 s with the consistent durations of 20 s for each of them (S2); and at the elapsed time of 50 s, 100 s, and 150 s with the respective durations of 10 s, 20 s, and 30 s (S3). In the last scenario, an outlier with significant measurement noise was simulated. The measurement noise was set to a relatively high value of $\text{diag}(1, 1, 0.1, 0.1, 0.1, 0.1)$ —equal to 1000 times of initial measurement noise—at the elapsed time of 150 s with the duration of 20 s (S4).

As examples, Fig. 2 demonstrates the displacement in surge influenced by the faulty sensors or large-amplitude measurement noises in S1, S2, S3, and S4. In Fig. 2a–c, because the sensor was completely faulty, the displacement values dropped to zero and recovered to normal values when the sensor resumed normal operations. In Fig. 2d, as additional measurement noises were added into the displacement data, large fluctuations of displacement values occurred and lasted until additional measurement noises were removed.

To evaluate the performance of the MUKF algorithm, the root mean square error (RMSE) was introduced to assess the estimation errors. The RMSE values of the three degrees of freedom (surge, sway, and yawing angle) are defined as RMSE_1 , RMSE_2 , RMSE_3 :

$$\left\{ \begin{array}{l} \text{RMSE}_1 = \sqrt{\frac{\sum_{j=1}^n (y_j - \hat{y}_j)^2}{n}} \\ \text{RMSE}_2 = \sqrt{\frac{\sum_{j=1}^n (x_j - \hat{x}_j)^2}{n}} \\ \text{RMSE}_3 = \sqrt{\frac{\sum_{j=1}^n (\psi_j - \hat{\psi}_j)^2}{n}} \end{array} \right. \quad (30)$$

where y_j , \hat{y}_j , x_j , \hat{x}_j , ψ_j , and $\hat{\psi}_j$ are the state values (predicted values) of surge, sway, and yawing angle, respectively. Note that the index RMSE has been commonly used in literature to represent the accuracy of the system to predict ship motion states such as [34].

As a reference, the UKF algorithm was also implemented to estimate the ship motion variables, and the results were compared to those from MUKF algorithm.

5.3 Sensitivity analysis

To demonstrate the MUKF's performance regarding its stability and convergence, a parameter sensitivity analysis was

conducted by significantly extending the basic outlier scenarios for Ship 1 presented in Sect. 5.2.

To assess the influence of sensor faulty duration on the performance of MUKF, single sensor fault was set to occur at the elapsed time of 50 s and lasted for 20 s (S1-1), 30 s (S1-2), 40 s (S1-3), 50 s (S1-4), and 60 s (S1-5) in S1 series; while for S3 series, multiple sensor faults were set at (50 s, 100 s, 150 s) with the respective durations of (10 s, 20 s, 30 s), (15 s, 25 s, 35 s), (20 s, 30 s, 40 s), (25 s, 35 s, 45 s), and (30 s, 40 s, 50 s). They were labeled as S3-1, S3-2, S3-3, S3-4, and S3-5.

For S2 series, to assess the influence of sensor faulty timing on the performance of MUKF, multiple sensor faults were set to occur at (50 s, 100 s, 150 s), (100 s, 150 s, 200 s), (150 s, 200 s, 250 s), and (200 s, 230 s, 300 s). They were labeled as S2-1, S2-2, S2-3, and S2-4.

For S4 series, to assess the noise extent on the performance of MUKF, the ratios of measurement noise to initial measurement noise were set to 100, 400, 700, 1000, 1300, and 1600 at the elapsed time of 150 s with the duration of 20 s. They were labeled as S4-1, S4-2, S4-3, S4-4, S4-5, and S4-6.

The RMSEs of the three degrees of freedom (surge, sway, and yawing angle) of all the scenarios were calculated and compared to assess the stability performance of the developed MUKF algorithm.

In addition, the convergence performance of the MUKF algorithm was analyzed on the simulated scenarios in terms of the algorithm running time which closely equals the convergence time.

6 Results

6.1 Typical scenarios

Figure 3 shows the comparisons of the estimated displacement values (surge, sway, and yawing angle) by the UKF and MUKF and corresponding theoretical values in S1, S2, S3, and S4. Regardless of the displacement type (surge, sway, or yawing angle), both the UKF and MUKF estimated good displacement values when no outlying data appeared. However, the displacement values predicted by the UKF departed significantly from the theoretical values in the outlier period: (a) the surge and sway values dropped to zero in S1, S2, and S3; (b) the yawing angle values dropped to around -0.67 radians with minor fluctuations in S1, S2, and S3; (c) the surge, sway, and yawing angle values fluctuated highly in S4. For the MUKF, the linear correlation coefficient between two variables (estimated vs. theoretical) equals more than 0.99 with r -squared values more than 0.99 for all scenarios (S1–S4), regardless of displacement type, indicating that the

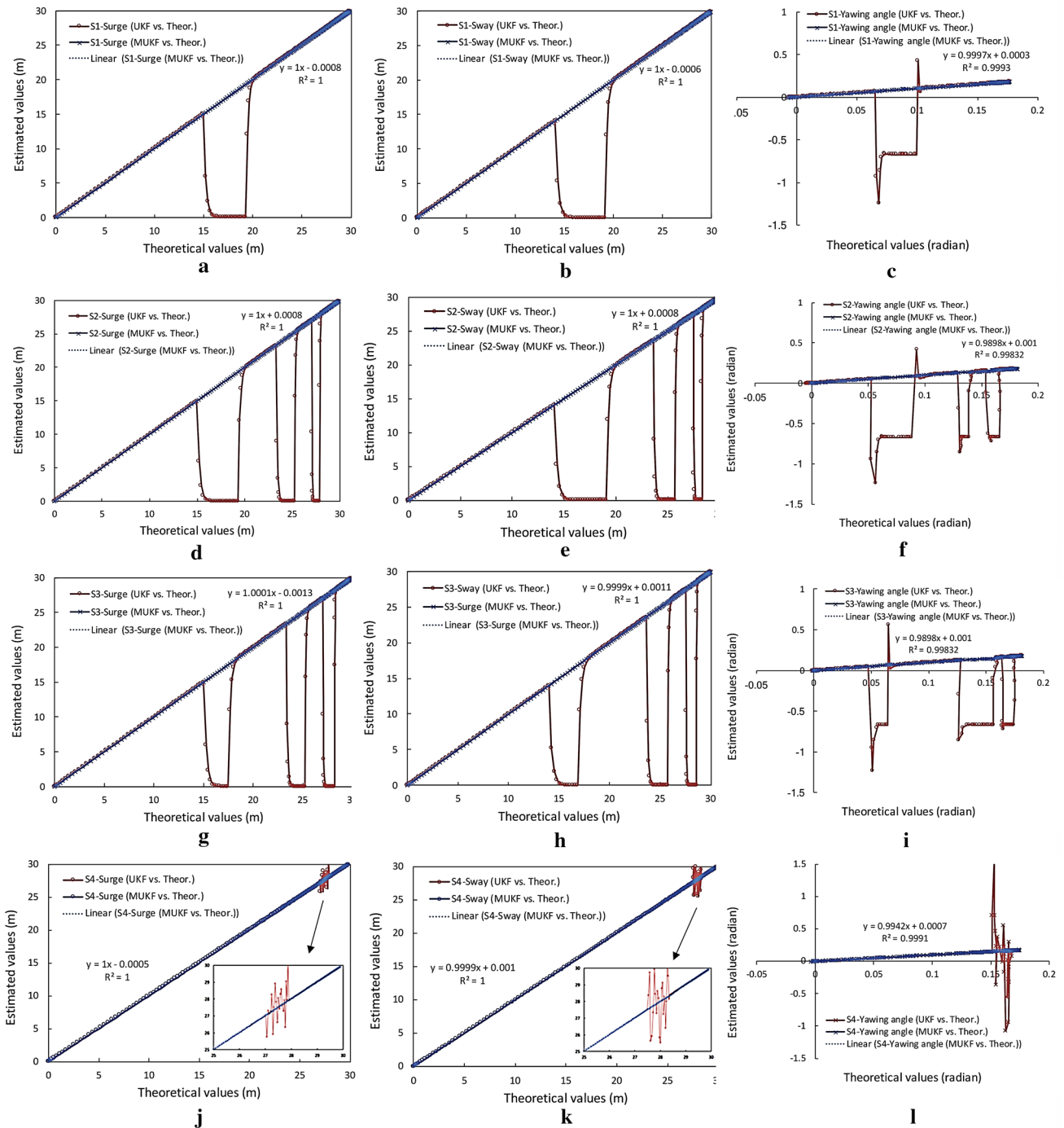


Fig. 3 The correlation of estimated displacement values and the theoretical values in different scenarios

MUKF estimated ship displacement values that are close to the theoretical values. For Ship 2, the result patterns are similar and are thus not shown.

The estimation errors of surge, sway, and yawing angle values produced by the MUKF and UKF algorithms with respect to elapsed time are shown in Fig. 4. The estimation error was calculated by subtracting the theoretical

displacement value from the estimated one. By utilizing the UKF, the estimation error dramatically increased by four to five orders of magnitude when the sensor faulted either completely or additional noises were added to the measurement. For the MUKF, on the other hand, the estimation errors remained small, and only marginal differences between estimated values and theoretical values were observed for all

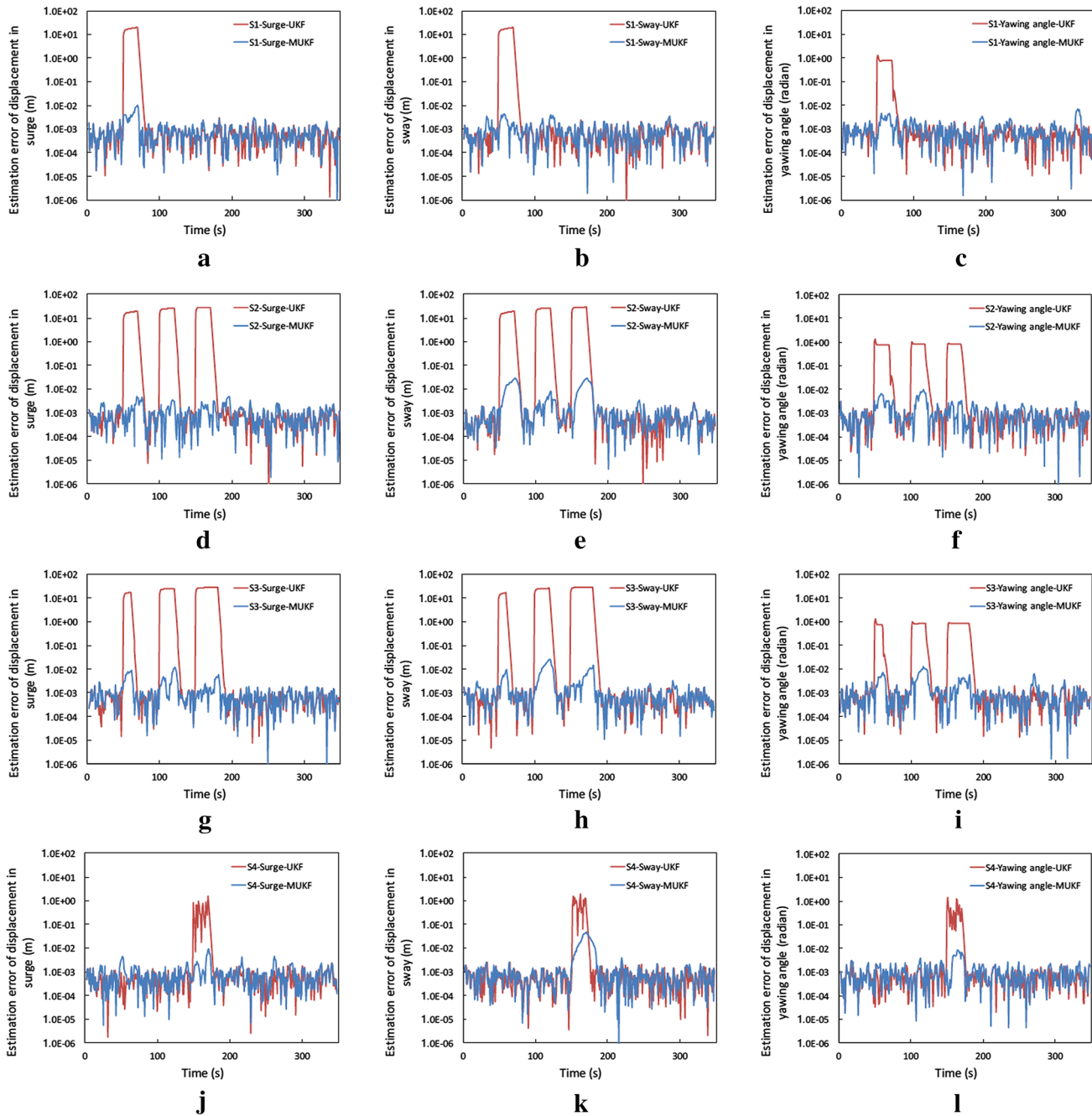


Fig. 4 Estimation error results of surge, sway, and yawing angle displacement in S1, S2, S3, and S4

scenarios (S1–S4), regardless of displacement type. For Ship 2, the result patterns are similar and are therefore not shown.

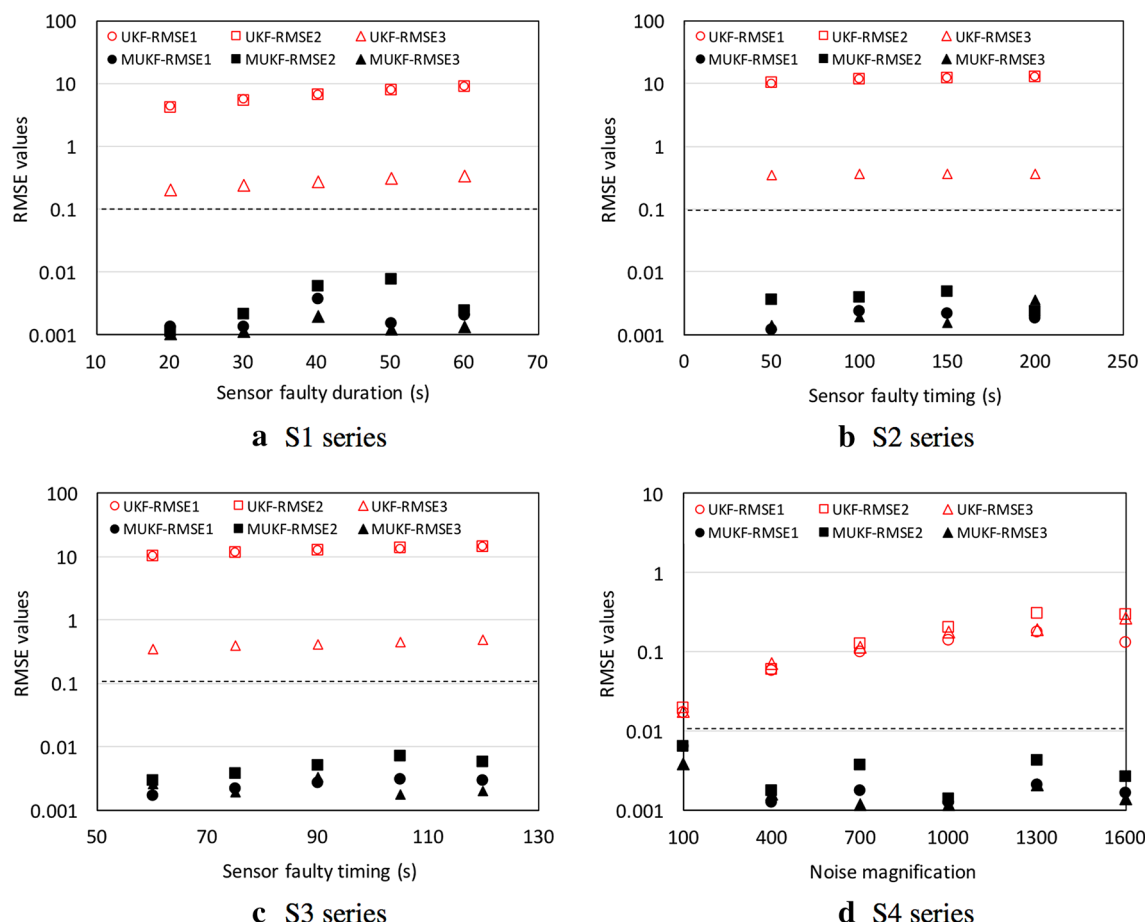
Interestingly, the MUKF has a distinct characteristic that differentiates it from the UKF. Once the sensor faulted, for the UKF, the estimation error of all displacement variables immediately jumped by several orders of magnitude to the summit, while for the MUKF, the estimation error did not reach the summit for several to tens of seconds; it also declined more gradually than that for the UKF. This delayed

reaction in the estimation error of ship motion states as a result of the MUKF algorithm will be discussed in Sect. 7.

The estimation accuracy of the UKF and MUKF can also be revealed by comparing the RMSEs of the displacement values of surge, sway, and yawing angle in Table 4. For Ship 1 (Ship 2), the RMSEs of surge, sway, and yawing angle estimated by the UKF are 29–6969 (23–5421) times higher than those estimated by the MUKF, which produced negligible estimation errors.

Table 4 Results of RMSEs of estimated UKF and MUKF

Scenarios	Algorithm	Ship 1			Ship 2		
		RMSE1 (surge)	RMSE2 (sway)	RMSE3 (yawing angle)	RMSE1 (surge)	RMSE2 (sway)	RMSE3 (yawing angle)
S1	UKF	4.1908	4.0891	0.2001	4.1888	4.0913	0.2001
	MUKF	0.0016	0.0012	0.0015	0.0012	0.0041	0.0013
S2	UKF	9.7559	9.8457	0.3455	9.7572	9.8605	0.3476
	MUKF	0.0014	0.0068	0.0020	0.0018	0.0049	0.0014
S3	UKF	10.3863	10.5292	0.3544	10.3869	10.5254	0.3543
	MUKF	0.0022	0.0045	0.0025	0.0021	0.0052	0.0026
S4	UKF	0.1486	0.2280	0.1439	0.1576	0.1252	0.1464
	MUKF	0.0014	0.0079	0.0017	0.0016	0.0055	0.0022

**Fig. 5** Results of sensitivity analysis for S1, S2, S3, and S4 series regarding the RMSE values

6.2 Sensitivity analysis

Figure 5 presents the results of sensitivity analysis for S1, S2, S3, and S4 series regarding the RMSE values. The convergence time of MUKF algorithm is shown in Table 5.

For S1 and S3 series, the increase of sensor faulty duration caused higher RMSE values produced from the UKF algorithm, and these values are more than 10 times higher than the RMSE values produced from the MUKF algorithm.

Table 5 Convergence time of MUKF algorithm for S1, S2, S3, and S4 series

S1 series	Conver-gence time (s)	S2 series	Conver-gence time (s)	S3 series	Conver-gence time (s)	S4 series	Conver-gence time (s)
S1-1	1.0	S2-1	1.0	S3-1	1.0	S4-1	1.1
S1-2	1.0	S2-2	1.0	S3-2	1.0	S4-2	1.1
S1-3	1.0	S2-3	1.0	S3-3	1.0	S4-3	1.0
S1-4	1.1	S2-4	1.1	S3-4	1.1	S4-4	1.1
S1-5	1.0			S3-5	1.0	S4-5	1.1
						S4-6	1.1

For S2 series, the sensor faulty timing caused little influence on RMSE values produced either from the UKF algorithm or from the MUKF algorithm. However, the RMSE values produced from the UKF algorithm are approximately 50 times higher than those produced from the MUKF algorithm.

For S4 series, the increase of noise magnification from 100 to 1600 caused up to 15 times higher RMSE values produced from the UKF algorithm but caused no increase of RMSE values produced from the MUKF algorithm.

All the simulated scenarios with outliers present short running time that is less than 1.1 s and yield no divergence, indicating the great convergence performance of the MUKF algorithm.

In view of the above results, the stability of MUKF algorithm can be proven.

7 Discussion

7.1 Effectiveness of the outlier detection function

To avoid manually tuning the parameter of the function, we assumed a chi square distribution for the outlier detection function values and pre-set the significance level as 0.01. Accordingly, a threshold chi square value of 11.345 was obtained for three-DOF. Although a significance level of 0.01 is a commonly used value, we nevertheless had to justify our use of this level because the threshold values $\chi^2_{\text{threshold}}$ in Eq. (27) are critical for us to judge whether an outlier occurs in the measurement system. Table 6 shows the influence of significance levels (0.005, 0.01, 0.025, and

0.05) and their corresponding chi square threshold values (12.838, 11.345, 9.348, and 7.815) on the estimation error in Scenario 1 for the simulation of Ship 1 and Ship 2.

Results show that RMSE values of different displacement types are rather small, regardless of the investigated significance levels, indicating the accuracy of the MUKF algorithm in estimating ship motion states. Studies such as [39] also employed the RMSE index to assess the accuracy of an algorithm. In the study [39], the authors reported a satisfactory prediction accuracy of the grey online-sequential-extreme-learning-machine algorithm with a RMSE value of 0.4515 for the prediction of ship roll motion states.

More importantly, results show that RMSE values are insensitive to the chi square threshold values and corresponding significance levels. This result indicates that the commonly used significance level of 0.01 is effective and rigorous to be used in the outlier detection function, which provides a basis to produce an adaptive and relatively robust MUKF algorithm. Further studies can be carried out to develop a universal function to detect outliers that can be used in a large variety of applications for detecting abnormalities, such as the presence of outliers in a navigation system.

7.2 Performance of the MUKF

The performance of the MUKF was revealed by filtering a single outlier (S1 and S4) and multiple outliers (S2 and S3) and estimating the main ship motion displacement variables—surge, sway, and yawing angle—when the measurements are abnormal. The proposed algorithm is superior to

Table 6 Influence of significance level on the estimation error of MUKF algorithm

Significance level	Ship 1			Ship 2		
	RMSE1	RMSE2	RMSE3	RMSE1	RMSE2	RMSE3
0.005	0.0025	0.0020	0.0020	0.0013	0.0011	0.0014
0.010	0.0027	0.0015	0.0030	0.0015	0.0020	0.0011
0.025	0.0020	0.0093	0.0016	0.0015	0.0016	0.0010
0.050	0.0021	0.0020	0.0024	0.0010	0.0031	0.0012

the UKF in spotting faults in the measurement system and producing a good estimation of ship state variables. This result was consistent for different ship displacement variables (surge, sway, and yawing angle) among different faulty measurement systems (S1, S2, S3, and S4) for different ships (Ship 1 and Ship 2). The sensitivity analysis also reveals that the great stability and convergence performance of the developed MUKF algorithm. Because only an outlier detection function was embedded in the regular UKF algorithm to judge whether outliers occur and because few steps were added in the UKF algorithm to update the filter gain and calculate state and covariance estimation as shown in Fig. 1, the developed MUKF algorithm is still computation-efficient and easy to implement.

The good performance of the MUKF estimation is mainly attributed to the effective detection of outliers—as discussed in Sect. 7.1. Once the outlying data are detected, the measurement residual in Eq. (26) is identified and the corresponding covariance matrix of the measurement noise and the predicted measurement, and the filter gain will be corrected for avoiding their dramatic changes. However, for the UKF, the outliers could cause large changes in the filter gain and thus the estimation of ship motion states. Therefore, compared with the MUKF, the UKF failed to eliminate the significant impact of outliers on the prediction of ship motion state, resulting in a high deviation of predicted values from the theoretical values.

For dealing with measured data with multiple outliers occurring in a consecutive sequence, the performance of the MUKF algorithm was still capable of eliminating the impact of each outlier if we analyze the results of S2 and S3 in Fig. 4, because the MUKF algorithm can independently eliminate the impact of each outlier without bringing in a residual impact from the preceding outlier.

In Eq. (28), a moving window was introduced to modify the covariance matrix when the outlier detection function spotted the outlying data. This moving window was able to moderate the extreme change in the covariance values of measurement noises and thus moderate the extreme change of ship motion states that were produced by the UKF. As a consequence, for the state variable values estimated by the MUKF, the state estimation errors gently increased up to the summit and gently decreased to the normal values when the outlier was absent. Use of the MUKF shortened the period during which the outliers impacted the estimation of ship motion states, compared to the results from UKF. To the best of our knowledge, this observation was first present in our study. In a practical case in which a system component suddenly fails and the other components are working based on the estimated state values of the malfunctioned component, those components may still operate for several seconds until the maximum estimated values exceed the threshold values. These several seconds

can become a warning period for us to find a reasonable solution to deal with the faulty components.

Most of the existing outlier robust estimators in literature can only be used to estimate the ship state variables by analyzing linear motion data [20–27]. The new MUKF algorithm can be potentially used to assess the state variables of ship motion which is nonlinear and dynamic. In addition, it is easier to implement MUKF algorithm with economic computations. To the best of our knowledge, there has been no ship motion experiment data with outliers published in literature. While, it is worth conducting a lab test or field experiment to verify our MUKF algorithm in future. We believe that our results support a collective awareness of ship motion outlier and its impact on ship motion state estimation and prediction. The new MUKF algorithm can support continual improvement of ship state prediction in real ocean conditions where unanticipated disturbances could induce the measurement of ship motion with outliers.

Our study is to provide a new algorithm for estimating ship motion states by analyzing the sensor signals that could be subjected to the influence of sensor faults or environment interference. There are uncountable scenarios that could cause the above unexpected sensor signals in the simulations. However, we conducted the simulation based on the two most possibly occurred scenarios. A sensor failure, in the worst case, could be the case where no sensor signal can be detected, for example, due to power failures on ships. It is also very normal to observe the signal outliers due to the environment noise (e.g., unexpected big wave).

The accurate estimation of ship state variables by the developed MUKF algorithm in this paper is important because it can truly reflect the dynamics of the ship so that the motion of ships can be properly monitored and recorded during the measurement. Inaccurate estimates of a ship motion state may result in severe security issues or other adverse consequences such as economic loss. Besides in the application of ship state estimation, the MUKF algorithm is also potentially used in many other control and signal processing applications such as underwater navigation systems where the acoustic data are frequently influenced by outlying data.

8 Conclusions

The state estimation of sensor signals with measurement outliers was studied, and a robust estimation solution was presented. An outlier detection function was introduced to modify the covariance matrix of measurement noise and the filter gain in the UKF algorithm. Consequently, a modified UKF (MUKF) was proposed to estimate ship motion states including surge, sway, and yawing angle values with elapsed

time. A simulation of ship motion with two ship models in three scenarios with sensor failures and one scenario with measurement noise was conducted followed by a sensitivity analysis. The conclusions of this simulation are as follows:

- The influence of significance level between 0.005 and 0.05 and the chi square threshold values on the estimation error of the MUKF algorithm was insignificant and manual parameter tuning was avoided in the MUKF algorithm.
- The MUKF algorithm accurately estimated all the investigated dynamic ship motion states (surge, sway, and yaw), regardless of the outlying scenarios.
- The impact period of outliers on the estimation of a ship motion state by the MUKF was slightly shorter than that of the UKF due to the moving window set to modify the covariance matrix of measurement noise.
- The MUKF algorithm shows a good stability and convergence performance based on the parameter sensitivity analysis.

Acknowledgements The research work described in this paper was supported by National Natural Science Foundation of China (Project No. 61503091). We also thank Paper going for its linguistic assistance during the preparation of this manuscript.

Compliance with ethical standards

Conflict of interest The authors declare no conflict of interest.

References

- Pascoal R, Perera LP, Soares CG (2017) Estimation of directional sea spectra from ship motions in sea trials. *Ocean Eng* 132:126–137
- Nielsen UD, Stredulinsky DC (2012) Sea state estimation from an advancing ship—a comparative study using sea trial data. *Appl Ocean Res* 34:33–44
- Iseki T, Terada D (2003) Study on real-time estimation of the ship motion cross spectra. *J Mar Sci Technol* 7(4):157–163
- Wu M, Hermundstad OA (2002) Time-domain simulation of wave-induced nonlinear motions and loads and its applications in ship design. *Mar Struct* 15:561–597
- Watanabe I, Soares CG (1999) Comparative study on the time-domain analysis of non-linear ship motions and loads. *Mar Struct* 12:153–170
- Lajic Z, Blanke M, Nielsen UD (2009) Fault detection for shipboard monitoring—Volterra Kernel and Hammerstein model approaches. In: Proceedings of 7th IFAC Symposium on Fault Detection, Supervision and Safety of Technical Processes, Barcelona, Spain 42(8):24–29
- Kalman RE (1960) A new approach to linear filtering and prediction problems. *J Basic Eng-T Asme* 82:35–45
- Cooper WS (1986) Use of the Kalman filter in signal processing to reduce beam requirements for alpha-particle diagnostics. *Rev Sci Instrum* 57:1846–1848
- Dove MJ (1977) Kalman filter techniques in marine integrated navigation systems. *J Navigation* 30:135–145
- Yan Y, Shi YC, Ma ZQ (2011) Moving vehicle tracking based on Kalman filter. *Appl Mech Matl* 71:3950–3953
- Julier SJ, Uhlmann JK, Durrant-Whyte HF (1995) A new approach for filtering nonlinear systems. In: Proceedings of the American Control Conference, IEEE, Seattle, USA, 3:1628–1632
- Julier SJ, Uhlmann JK, Durrant-Whyte HF (2000) A new method for nonlinear transformation of means and covariances in filters and estimators. *IEEE Trans Autom Control* 45:477–482
- Julier SJ, Uhlmann JK (2004) Unscented filtering and nonlinear estimation. *Proceedings of the IEEE* 92:401–422
- Peng Y, Han J, Wu Z (2007) Nonlinear backstepping design of ship steering controller: using unscented Kalman filter to estimate the uncertain parameters. In: Proceedings of the IEEE International Conference on Automation and Logistics, Jinan, China
- Peng Y, Han J, Song Q (2007) Tracking control of underactuated surface ships: using unscented Kalman filter to estimate the uncertain parameters. In: Proceedings of the 2007 IEEE International conference on Mechatronics and Automation, Harbin, China
- Barnett V, Lewis T (1994) Outliers in statistical data, 3rd edn. Wiley, New York
- Lajic Z, Blanke M, Nielsen UD (2010) Fault isolation for shipboard decision support. In: Proceedings of 7th IFAC Symposium on Intelligent Autonomous Vehicles, Lecce, Italy 43(16):413–418
- Drevelle V, Bonnifait P (2016) Interval-based fast fault detection and identification applied to radio-navigation multipath. *Int J Adapt Control Signal Process* 30:154–172
- George N, Panda G (2015) Development of a novel robust identification scheme for nonlinear dynamic systems. *Int J Adapt Control Signal Process* 29:385–406
- Palma DD, Indiveri G (2017) Output outlier robust state estimation. *Int J Adapt Control Signal Process* 31:581–607
- Masreliez C, Martin R (1977) Robust Bayesian estimation for the linear model and robustifying the Kalman filter. *IEEE Trans Autom Control* 22:361–371
- Masreliez C (1975) Approximate non-Gaussian filtering with linear state and observation relations. *IEEE Trans Autom Control* 20:107–110
- Doraiswami R (1976) A decision theoretic approach to parameter estimation. *IEEE Trans Autom Control* 21:860–866
- Morris J (1976) The Kalman filter: a robust estimator for some classes of linear quadratic problems. *IEEE T Inform Theory* 22:526–534
- Hajiyev C, Caliskan F (2000) Sensor/actuator fault diagnosis based on statistical analysis of innovation sequence and Robust Kalman filtering. *Aerospace Sci Technol* 4:415–422
- Soken HE, Hajiyev C (2010) Pico satellite attitude estimation via robust unscented Kalman filter in the presence of measurement faults. *ISA Trans* 49:249–256
- Hajiyev C, Ersin H (2013) Robust adaptive Kalman filter for estimation of UAV dynamics in the presence of sensor/ actuator faults. *Aerospace Sci Technol* 28:1–8
- Durovic ZM, Kovacevic BD (1999) Robust estimation with unknown noise statistics. *IEEE Trans Autom Control* 44:1292–1296
- Ting JA, Theodorou E, Schaal S (2007) A Kalman filter for robust outlier detection. In: Proceedings of Intelligent Robots and Systems, IEEE, San Diego, USA, pp 1514–1519
- Huber PJ (2011) Robust statistics. In: Miodrag L (ed) International encyclopedia of statistical science. Springer, Berlin pp 1248–1251, ISBN: 978-3-642-04897-5
- Salvesen N, Faltinsen O (1970) Ship motions and sea loads. *Soc Naval Archit Mar Eng* 6:1–30
- Wei S, Liang L, Zhang H (2006) Influence of sway motion on passive anti-rolling tank. *J Mar Sci Appl* 5:17–22
- Du J, Hu X, Krstić M, Sun Y (2016) Robust dynamic positioning of ships with disturbances under input saturation. *Automatica* 73:207–214

34. Xiong K, Wei CL, Liu LD (2015) Robust multiple model adaptive estimation for spacecraft autonomous navigation. *Aerospace Sci Technol* 42:249–258
35. Fossen TI, Strand JP (1999) Passive nonlinear observer design for ships using Lyapunov methods: full-scale experiments with a supply vessel. *Automatica* 35:3–16
36. Snijders JG, Van Der Woude JW, Westhuis J (2005) Nonlinear observer design for dynamic positioning. In: *dynamic Positioning Conference-control system I*
37. Fossen TI (2002) Marine control systems: guidance, navigation and control of ships, rigs and underwater vehicles. *Marine Cybernetics*, Trondheim, pp 537–564
38. Greenwood PE, Nikulin MS (1996) A guide to chi-squared testing. John Wiley & Sons, Hoboken, ISBN: 978-0-471-55779-1
39. Yin JC, Zou ZJ, Xu F, Wang NN (2014) Online ship roll motion prediction based on grey sequential extreme learning machine. *Neurocomputing* 129:168–174

Publisher's Note Springer Nature remains neutral with regard to jurisdictional claims in published maps and institutional affiliations.